International Journal of Thermophysics, Vol. 27, No. 6, November 2006 (© 2006)
DOI: 10.1007/s10765-006-0104-8

A Multiparameter Thermal Conductivity Equation for 1,1-Difluoroethane (R152a) with an Optimized Functional Form[1]

G. Scalabrin,[2,3] P. Marchi,[2] and F. Finezzo[2]

The application of an optimization technique to the available experimental data has led to the development of a new multiparameter equation $\lambda = \lambda(T, \rho)$ for the representation of the thermal conductivity of 1,1-difluoroethane (R152a). The region of validity of the proposed equation covers the temperature range from 220 to 460 K and pressures up to 55 MPa, including the near-critical region. The average absolute deviation of the equation with respect to the selected 939 primary data points is 1.32%. The proposed equation represents therefore a significant improvement with respect to the literature conventional equation. The density value required by the equation is calculated at the chosen temperature and pressure conditions using a high accuracy equation of state for the fluid.

KEY WORDS: 1,1-difluoroethane; HFC-152a; multiparameter equations; R152a; thermal conductivity; transport property correlation techniques.

1. INTRODUCTION

Among the alternative refrigerants for the replacement of chlorofluorocarbons, 1,1-difluoroethane (R152a) is one of the most promising fluids, due to its favorable characteristics with respect to the environment; in fact, it has a null ozone-depletion potential and the lowest global-warming potential of the hydrofluorocarbon family. Moreover, it has low toxicity,

[1]Paper presented at the Seventeenth European Conference on Thermophysical Properties, September 5–8, 2005, Bratislava, Slovak Republic.

[2]Dipartimento di Fisica Tecnica, Università di Padova, via Venezia 1, I-35131 Padova, Italy.

[3]To whom correspondence should be addressed. E-mail: gscala@unipd.it

high chemical stability, and thermodynamic properties suitable for technical applications.

As a consequence of its technical interest, the thermodynamic and thermophysical properties of R152a have to be known with an accuracy as high as possible. At present, both a highly accurate fundamental equation of state (EoS) with a wide validity range [1] and a crossover model for the critical region [2] are available for this fluid and all of its thermodynamic properties can then be calculated with high precision. An accurate viscosity model with a wide region of validity was recently proposed [3], and the present work is focused on the modeling of the thermal conductivity.

A brief summary of the different approaches reported in the literature for the representation of the transport properties was presented in previous studies [4, 5]. In particular, the state-of-the-art technique for the development of dedicated transport property equations is noted here. Such a method, in the following referred to as 'conventional', is based on the residual concept and it considers each transport property function as composed of three parts: the zero-density term, the excess term, and the critical enhancement term [6]. For the case of thermal conductivity λ, the obtained equation has the general form $\lambda = \lambda(T, \rho)$, where the independent variables are the temperature T and the density ρ.

Since the controlling variables for experimental measurements and for technical applications are the temperature T and the pressure P, an accurate equation of state is needed for the variable conversion from (T, P) to (T, ρ). This is a necessary condition for all transport property equations covering the whole fluid surface, unless implicit functional forms are used [7].

Even if theoretically-based expressions are assumed for some parts of the transport property equations in conventional format, the technique is, however, to some extent, correlative and the development of the equation for the considered fluid requires experimental data of the studied transport property over the whole range of interest. Some difficulties in the regression procedure are also found [4, 5].

As alternatives to the conventional procedure, some totally correlative techniques were also developed [3–5, 8–15]. Among the others, the technique for optimizing the functional form of multiparameter equations of state, developed by Setzmann and Wagner [16], proved to be a powerful function approximator suitable to develop a transport property equation directly from the experimental data. The method was previously used with successful results for the modeling of viscosity [3, 4, 14] and of thermal conductivity [5, 15], and the present work deals with the application of this modeling technique to the thermal conductivity representation of R152a. For the sake of precision, it should be noted that the algorithm of

Setzmann and Wagner was already applied to transport property modeling of oxygen in 1990 [7], but in that case the model format and its representation capability were completely different from the present one.

The thermal conductivity equation for R152a developed by Krauss et al. [17] in the conventional format was used here for comparisons.

2. EXPERIMENTAL DATA

From the experimental point of view, the thermal conductivity of R152a has been extensively studied only in recent times, mainly in the last decade; nevertheless, a reasonable amount of measurements from independent researchers can be found in the literature. The available datasets, grouped according to their phase, are presented in Table I together with the validation of the new equation. In the present work, *liquid* refers to a thermodynamic state where the temperature is lower than the critical temperature and the pressure is higher than the saturation pressure; *vapor* is characterized by a pressure lower than the saturation value or, at a supercritical temperature, by a pressure lower than the critical pressure; *supercritical* indicates that both temperature and pressure are higher than the respective critical values.

Table I reports in the column 'NPT' the number of experimental points in each dataset; the individual ranges of the independent variables and the adopted measurement method are also given. The data are divided according to their classification as primary (I) or secondary (II), as it results from the screening procedure discussed in Section 3.3. The primary data were used in the regression of the thermal conductivity equation, whereas the secondary data, due to their lower accuracy, were considered only for validation to check the performance of the model with respect to the most comprehensive data base. The other parts of Table I will be explained in the following.

The primary data distribution in the T, P plane is shown in Fig. 1, from which one can see that some regions are widely investigated, whereas the vapor phase at temperatures lower than 250 K and the liquid phase at temperatures lower than 300 K and pressures greater than 25 MPa are not documented.

The temperatures of the experimental data were converted, when necessary, to the International Temperature Scale of 1990 (ITS-90) [35].

Table I. Experimental Data and Their Deviations from the New Thermal Conductivity Equation, Eq. (12). Data are within the Limits of Validity of Eq. (12)

Ref.	First Author	Phase[a]	NPT	NPT Range	T Range (K)	P Range (MPa)	Meas. Method[b]	AAD (%)	Bias (%)	MAD (%)	Class	$u_{\%}$ (%)
Liquid phase												
18	Assael	l	37	37	253–333	0.5–22.4	HW, T	0.81	−0.44	2.51	I	0.5
18	Assael	sl	5	5	253–333	–	HW, T	1.24	−0.61	2.39	I	0.5
19	Geller	l	108	108	306–382	1.1–6.9	HW, S	1.56	0.73	10.50	I	2.0
20	Gross	l	44	44	253–363	0.2–6.2	HW, T	1.96	1.86	5.01	I	1.6
21	Gurova	l	38	31	224–294	0.8–18.0	HW, T	1.97	−1.97	3.40	I	0.5
21	Gurova	sl	5	4	224–294	–	HW, T	1.57	−1.57	2.71	I	0.5
22	Kim	l	25	25	223–323	2.1–20.1	HW, T	0.59	−0.43	1.49	I	2.0
22	Kim	sl	5	5	223–323	–	HW, T	0.36	0.05	0.71	I	2.0
23	Le Neindre	l	252	252	307–378	1.0–55.0	CC, S	0.50	0.05	4.11	I	1.5
	Primary			511				0.98	0.15	–		
24	Grebenkov	l	72	72	294–381	0.8–20.0	CC	5.44	−5.44	9.96	II	–
25	Gross	sl	24	24	253–313	–	HS	3.93	3.93	6.31	II	–
26	Kraft	sl	16	16	279–386	–	DLS	5.13	−0.52	25.44	II	–
27	Kruppa	l	27	27	367–386	3.5–11.4	DLS	6.80	−4.69	18.11	II	–
27	Kruppa	sl	49	49	293–386	–	DLS	9.99	7.22	64.79	II	–
28	Tsvetkov	l	11	8	221–300	7.7–8.6	CC, T	2.02	2.02	2.95	II	–
29	Vargaftik	l	33	33	305–380	1.1–4.0	CO	0.96	0.24	5.91	II	–
30	Yata	l	20	20	266–343	1.4–30.6	HW, T	3.76	−2.12	9.50	II	–
	Total		771	760				2.45	−0.03	–		
Vapor phase												
31	Afshar	v	13	10	280–460	0.1	HW	2.14	0.58	3.81	I	3.0
19	Geller	v	19	19	305–433	0.1	HW, S	0.91	0.15	4.05	I	2.0
20	Gross	v	40	40	254–354	0.1–2.3	HW, T	1.70	0.67	4.48	I	2.0
27	Kruppa	v	56	46	367–425	2.2–4.5	DLS	2.99	0.27	8.23	I	5.0
23	Le Neindre	v	48	48	298–456	0.1–4.5	CC, S	2.30	−0.50	9.12	I	1.5

Table I. Continued.

Ref.	First Author	Phase[a]	NPT	NPT Range	T Range (K)	P Range (MPa)	Meas. Method[b]	AAD (%)	Bias (%)	MAD (%)	Class	$u_{\%}$ (%)
32	Taxis-Reischl	v	54	54	277–400	0.0–2.4	HW, T	1.53	0.08	4.89	I	1.0
	Primary			217				2.02	0.12	–		
33	Hammerschmidt	v	5	4	303–423	0.1	PP	4.55	3.64	8.24	II	–
26	Kraft	sv	6	6	360–386	–	DLS	7.39	7.39	27.32	II	–
27	Kruppa	sv	30	30	348–386	–	DLS	17.51	−16.11	90.52	II	–
29	Vargaftik	v	13	10	280–460	0.2	CO	2.55	−2.55	5.37	II	–
34	Yin	v	14	14	279–349	0.1	HW, T	7.16	−7.16	8.67	II	–
	Total		298	281				4.10	−1.86	–		
Supercritical region												
27	Kruppa	sc	115	103	387–426	4.5–10.9	DLS	2.31	−0.64	6.28	I	5.0
23	Le Neindre	sc	108	108	391–455	5.0–41.0	CC, S	0.63	0.08	3.54	I	1.5
	Primary			211				1.45	−0.27	–		
24	Grebenkov	sc	6	6	398–399	10.0–20.0	CC	8.82	−8.82	9.51	II	–
	Total		229	217				1.65	−0.51	–		
Overall												
	Primary			939				1.32	0.05	–		
	Total		1298	1258				2.68	−0.52	–		

[a]Phase: l = liquid phase, sl = saturated liquid, v = vapor phase, sv = saturated vapor, sc = supercritical region.

[b]Measurement method: CC = coaxial cylinder; CC, S = coaxial cylinder steady-state; CC, T = coaxial cylinder transient; CO = compilation; DLS = dynamic light scattering; HS = hot strip; HW = hot wire; HW, S = hot wire steady-state; HW, T = hot wire transient; PP = parallel plate.

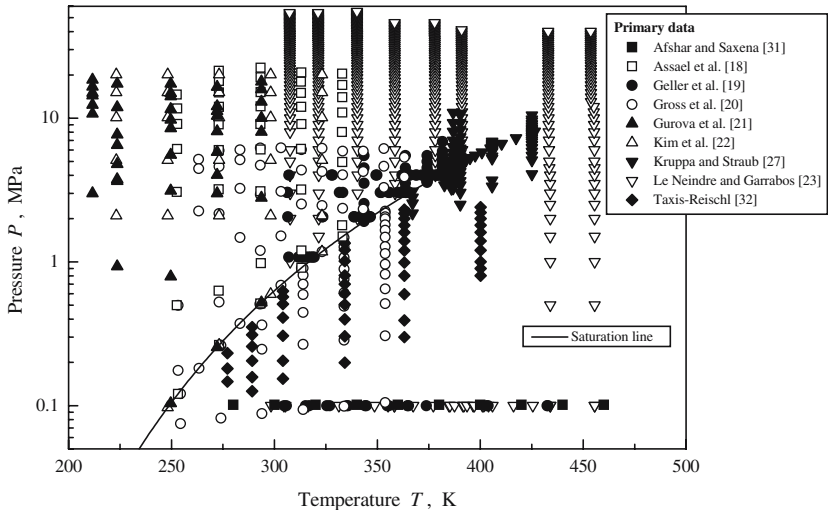

Fig. 1. Distribution of the data selected as primary data.

3. PROCEDURE FOR DEVELOPING THE NEW EQUATION FOR THERMAL CONDUCTIVITY

3.1. Fitting a Multiparameter Empirical Equation

The general form of an empirical multiparameter equation for the thermal conductivity of a pure fluid can be expressed as $\lambda = \lambda(T, \rho, \bar{n})$, where $\bar{n}$ represents the array of the individual coefficients to be fitted. The best set of values for the coefficients $\bar{n}$ is obtained by minimizing an objective function calculated from the experimental data as a sum of squares:

$$\chi^2(\bar{n}) = \sum_{i=1}^{N} \left(\frac{100}{u_{\%}} \cdot \frac{\lambda_{\text{exp}} - \lambda_{\text{calc}}(\bar{n})}{\lambda_{\text{exp}}} \right)_i^2 \tag{1}$$

where N is the total number of experimental points used in the regression and the subscripts exp and calc stand for experimental and calculated values, respectively.

In the objective function of Eq. (1), the deviations of the experimental points from the equation are weighted by their experimental uncertainty $u_{\%}$. The numerical values of $u_{\%}$, obtained by the claimed uncertainties given by the authors, are reported in the last column of Table I for the primary data used in the regression of the thermal conductivity equation. Kruppa and Straub [27] stated an uncertainty of 0.5–5% for their thermal diffusivity data considering the additional uncertainty for density and

isobaric heat capacity, see Eq. (9), an uncertainty of 5% was estimated for the thermal conductivity values of this dataset.

The minimization technique assumed for the present work is mainly based on the optimization algorithm developed by Setzmann and Wagner [16]. The starting point is constituted by a comprehensive function called 'bank of terms', i.e., a set of simple mathematical expressions whose summation is suitable to represent the required functional dependence. The algorithm, working on the basis of statistical criteria, selects the functional form yielding the best representation of the selected experimental data with the fewest number of terms.

The Setzmann and Wagner algorithm is a linear method and it can then be applied only to equations that are linear in the coefficients $\bar{n}$; for the present problem the flexibility of the empirical functional form was increased by coupling the algorithm with a nonlinear minimization method, skipping in this way the restrictions imposed by the linear method. The details of the fitting procedure are given in Section 3.3.

3.2. Bank of Terms

The bank of terms chosen for the optimization of the functional form is composed of a total of 285 terms; according to this choice, the most general form of the thermal conductivity equation can be written as

$$\lambda_r(T_r, \rho_r, \bar{n}, \bar{a}) = \sum_{i=0}^{12}\sum_{j=0}^{10} n_{ij} T_r^{i/2} \rho_r^j + e^{-5\rho_r^2} \sum_{k=0}^{12}\sum_{l=0}^{10} n_{kl} T_r^{k/2} \rho_r^l + n_c \lambda_{r,ce}(T_r, \rho_r, \bar{a}) \qquad (2)$$

with $j \neq 0$ when $i = 0$, and $l \neq 0$ when $k = 0$.

The reduced variables in Eq. (2) are defined as

$$\begin{aligned} T_r &= T/T_c \\ \rho_r &= \rho/\rho_c \\ \lambda_r &= \lambda/\Lambda_c \end{aligned} \qquad (3)$$

where the subscript c denotes the critical value. The actual critical values are used as reducing parameters for the temperature and the density, but this is not possible for the thermal conductivity because this quantity tends to infinity at the critical point [36]. The 'critical thermal conductivity' cannot be measured and it is therefore substituted by the parameter

Table II. Substance-Specific Parameters for the Target Fluid (R152a)

		Ref.
M (kg·mol^{-1})	0.066051	1
T_c (K)	386.411	2
P_c (MPa)	4.520	2
ρ_c (kg·m^{-3})	368.0	2
Λ_c (mW·m^{-1}·K^{-1})	2.72640	–

Λ_c, defined, for instance, in Ref. 7:

$$\Lambda_c = \frac{R^{5/6} P_c^{2/3}}{T_c^{1/6} M^{1/2} N_A^{1/3}} \tag{4}$$

The values of the molar mass M and of the critical parameters for the target fluid R152a are reported in Table II. The other quantities in Eq. (4) are the universal gas constant ($R = 8.314472\,\mathrm{J\cdot mol^{-1}\cdot K^{-1}}$), taken from Ref. 37, and Avogadro's number ($N_A = 6.0221353 \times 10^{23}\,\mathrm{mol^{-1}}$), taken from Ref. 38.

A bank of terms similar to Eq. (2), with the exclusion of the term $\lambda_{r,ce}$, was successfully used for the development of EoSs [39, 40] and of viscosity equations [3, 4, 14] for pure fluids. Furthermore, such a method is suitable for the representation of the background contribution of the thermal conductivity of a pure fluid, as was verified with some preliminary tests. A similar bank of terms was used also by Lemmon and Jacobsen [41] for modeling the residual contribution of viscosity and thermal conductivity equations for air and its pure components.

The enhancement of the thermal conductivity in the near-critical region is described by the critical term $\lambda_{r,ce}$:

$$\lambda_{r,ce}(T_r, \rho_r, \bar{a}) = \frac{\rho_r\, e^{-\frac{a_1}{\rho_r^{a_1}} - (a_2(T_r-1))^2 - (a_3(\rho_r-1))^2}}{\left\{\left\{\left[\left(1-\frac{1}{T_r}\right) + a_4\left((\rho_r-1)^2\right)^{\frac{1}{2a_5}}\right]^2\right\}^{a_6} + \left\{[a_7(\rho_r-\alpha)]^2\right\}^{a_8}\right\}^{a_9}} \tag{5}$$

for which

$$\alpha = \alpha(T_r) = 1 - a_{10}\,\mathrm{arccosh}\left\{1 + a_{11}\left[(1-T_r)^2\right]^{a_{12}}\right\} \tag{6}$$

The functional form in Eq. (5), empirically obtained with a trial-and-error procedure of regression on generated data of different fluids, is sufficiently flexible to follow the data trends, and it was already applied with satisfying

results for the cases of R134a [5] and carbon dioxide [15]. The parameters $\bar{a}$ and the multiplying coefficient n_c are regressed during the fitting procedure from experimental data of the target fluid.

In accordance with the behavior required for a critical enhancement term, the functional form given by Eqs. (5) and (6) diverges to infinity at the critical point; it is identically null at zero-density conditions and its numerical value decreases moving away from the critical point, with a rate depending on the parameters $\bar{a}$.

The function α lets the $\lambda_{r,ce}$ term assume, along isotherms at temperatures higher than the critical one, a maximum value at density values different from the critical, as the experimental data show. The purpose of α is then to make Eq. (5) non-symmetric with respect to critical density.

The coefficients a_4 and a_5, as for the corresponding parameters of the non-analytical terms in the EoS development [40], were fitted to density data for saturated liquid and saturated vapor near the critical point; the obtained coefficients were then rounded to values with only two decimal digits.

The bank of terms includes a single and very flexible critical enhancement term. Several simpler terms with different values of the parameters could also have been included, but in this second case unreasonable interactions among the terms may arise during the fitting procedure. In fact, the simultaneous presence in the equation of two or more terms with a similar peak behavior may result in unrealistic trends of the model to such a point to give negative values of thermal conductivity in some limited regions. On the other hand, it was verified that a single term with the form of Eq. (5) is sufficient for a satisfactory representation of the critical enhancement part of the thermal conductivity. This statement is confirmed by the results obtained for R134a [5], for carbon dioxide [15], and for the present fluid, as evidenced in the following.

3.3. Screening of Data and Fitting Procedure

Since the experimental datasets from the literature have different uncertainty levels and can be affected by systematic errors, a screening procedure is required to identify the data sources to include in the final regression. The present heuristic fitting technique can be used for this purpose: the screening and the fitting are performed through a series of steps following the selected procedure. The available thermal conductivity datasets for R152a were mainly measured in the last fifteen years, and the adopted experimental techniques are the most advanced; therefore, the accuracy of the data should be rather homogeneous.

A preliminary screening of the data was performed using the conventional equation for R152a from Krauss et al. [17] in order to identify the sources affected by large systematic errors. For each experimental point the error deviation Δ with respect to the equation was calculated as

$$\Delta = \frac{\lambda_{\text{exp}} - \lambda_{\text{calc}}}{\lambda_{\text{exp}}} \tag{7}$$

Some statistical indexes, used throughout the present work, are evaluated from the error deviation Δ: the average absolute deviation (AAD), the bias (Bias), and the maximum absolute deviation (MAD). These are defined as

$$\text{AAD}\ (\%) = \frac{100}{\text{NPT}} \sum_{i=1}^{\text{NPT}} |\Delta|_i \quad \text{Bias}\ (\%) = \frac{100}{\text{NPT}} \sum_{i=1}^{\text{NPT}} (\Delta)_i$$
$$\text{MAD}\ (\%) = 100\ \text{Max}\ |\Delta|_i \tag{8}$$

An error threshold with respect to the equation was chosen as an AAD of 5%. Each dataset was evaluated as a whole supposing that, apart from evident errors, all the points from the same set were obtained with a homogeneous uncertainty. The datasets from this first screening constitute the *preliminary* sources.

Considering the particular behavior of the thermal conductivity near the critical point, it was decided to separately screen the data inside and outside the near-critical region. The experimental points for which the critical enhancement contribution was greater than 3% of the overall thermal conductivity value were arbitrarily considered as *inside* the near-critical region; for this evaluation the critical enhancement contribution and the overall value were calculated from the conventional equation [17] at the (T, P) conditions of each experimental point.

A first regression was developed on the preliminary data *outside* the near-critical region using the optimization algorithm, but with the exclusion of the critical term $\lambda_{\text{r,ce}}$ from the bank of terms. A first selection of the primary sets in this region was obtained considering only sets with a threshold of 2–3% for the AAD and a low value for the bias. The choice of the primary datasets, on which the fitting is developed, was refined through successive regressions with the optimization algorithm. At each step some sets can be moved from primary to secondary, and *vice versa*, searching for the AAD values of the single primary sets to be as much as possible similar to the overall value for primary data and for the single bias values to be as close as possible to zero. At the end of the procedure, a group of sets with the smallest error deviations and statistically centered with respect to the multiparameter equation was obtained.

A similar procedure was applied to the preliminary data *inside* the near-critical region. In this case, the critical term $\lambda_{r,ce}$, Eqs. (5) and (6), with tentative coefficients $\bar{a}$ was added to the equation obtained in the previous section and the coefficients $\bar{a}$ and n_c were fitted using a nonlinear regression method. A first selection of primary sources was carried out also for this region.

Successively the term $\lambda_{r,ce}$, with updated coefficients, was included again into the bank of terms and a series of cycles, composed of the Setzmann and Wagner algorithm [16] followed by the non linear regression, was performed, each time updating the coefficients $\bar{a}$ of $\lambda_{r,ce}$ in the bank of terms. As described above, during this procedure the datasets can be moved from primary to secondary and *vice versa*, searching for a homogeneity of prediction accuracy with respect to the assumed primary sets.

At last, a stable selection of primary data was obtained from the screening procedure and the final version of the thermal conductivity equation for the whole surface was regressed from them. In the validation tables, the primary datasets are denoted by the symbol I, the secondary by II.

The availability of a conventional thermal conductivity equation for the fluid of interest is not a fundamental requirement for the present procedure, but it simply makes the screening easier. Therefore, even if no equation is available, at the beginning the procedure can be applied anyway. In fact, the use of the conventional equation for the preliminary screening of the experimental data sources reduces the subsequent screening efforts, but the screening could also be obtained using the optimization algorithm just from the first step on the whole database. On the other hand, the classification of each experimental point as falling inside or outside the near-critical region is essentially a rough procedure that could be alternatively performed with a simple equation in a predictive format.

Some comments about the final selection of primary data can be made. In fact, apart from a couple of older sets [30, 34], all the data measured with the transient hot wire technique [18, 20, 21, 22, 32] are included in the primary sets; this is not surprising, because the transient hot wire technique is considered the most reliable one for the measurement of the thermal conductivity of fluids. Also other datasets obtained with different versions of the hot wire technique [19, 31] are primary sets.

The data from Le Neindre and Garrabos [23] were measured a few years ago with a different method, i.e., the concentric cylinder technique. Even if such a method is considered less precise, its recent versions are probably more reliable than earlier ones, and then these data deserve to be included in the primary sets; moreover, they cover the widest range in both temperature and pressure.

The data from Kruppa and Straub [27] obtained with a dynamic light scattering technique have a lower accuracy with respect to other techniques, also due to the required conversion from thermal diffusivity to thermal conductivity value, see Section 3.4. In spite of this, they are the best data available in the critical region and then they were included as a primary set. The Kruppa and Straub data measured at saturation conditions, both in liquid and in vapor phase, show a much lower precision level and consequently were considered as secondary data.

In conclusion, the results of the screening procedure for the selection of primary datasets are consistent with the analysis based on the adopted experimental techniques.

3.4. Notes on Thermal Diffusivity Datasets

Among the datasets in the literature there are two sources [26, 27] which report thermal diffusivity D_T measurements instead of thermal conductivity. The relation between the two properties is expressed by

$$\lambda = \rho c_p D_T \tag{9}$$

where c_p is the isobaric heat capacity.

These datasets are the only ones available near the critical point and then, in order to consider such experimental points, the thermal diffusivity values were converted to thermal conductivity using Eq. (9). The required thermodynamic properties were calculated either from the Tillner-Roth EoS [1] or from the crossover model [2], as explained in Section 4.1.

The data of Kruppa and Straub [27] are presented with T and ρ as independent variables, instead of the used operative variables T and P; as a consequence, the densities for these points were assumed with the original values instead of recalculating them with the EoS at the (T, P) conditions. For the data at saturation from Kraft and Leipertz [26], both ρ and c_p were calculated by the appropriate thermodynamic model.

Since the critical values of temperature and density in Ref. 27 slightly differ from those assumed for R152a in the present work, Table II, the temperatures and densities of the data in this source were shifted in order to superimpose the critical points, similarly to what was formerly done in Ref. 17. This adjustment is necessary to avoid inconsistencies between the trends of the data and the model in the vicinity of the critical point. A similar shift was applied to temperatures for the data from Ref. 26.

The transformation from thermal diffusivity to thermal conductivity values increases the experimental error of the thermal conductivity data, since additional uncertainties on ρ and c_p are inevitably introduced.

Moreover, the properties near the critical point are difficult to measure and subject to greater uncertainties. As a consequence, some points belonging to these datasets were rejected during the fitting procedure because they were affected by very high errors; the accuracy of these sets is globally lower in comparison with other data sources.

4. NEW THERMAL CONDUCTIVITY EQUATION FOR R152A

4.1. Recommended Equation of State

The independent variables of the proposed thermal conductivity equation are temperature and density, but the controlling experimental variables are temperature and pressure. As a consequence, the development and the application of the thermal conductivity model require an EoS for the conversion from (T, P) to (T, ρ). In the present work, the fundamental EoS from Tillner-Roth [1] was used. Nevertheless, this equation is not suitable to accurately represent the thermodynamic properties in the critical region and consequently a theoretically based crossover model from van Pelt and Sengers [2], specialized for the critical region, was also assumed.

The application region of the crossover model is delimited by the following boundary:

$$T = a\rho^2 + b\rho + c \tag{10}$$

where

$$a = -\frac{T_c}{3\rho_c^2} \qquad b = \frac{3T_c}{4\rho_c} \qquad c = \frac{3}{4}T_c \tag{11}$$

and $365 \leq T/\mathrm{K} \leq 452.83$. Outside this boundary the Tillner-Roth EoS is adopted. The regions of application of the two models are shown in Fig. 2 on both the T, ρ and the P, T planes.

The overall thermodynamic EoS constituted by the two models was used for the calculation of the densities of the experimental points, given T and P, and for the transformation of the thermal diffusivity measurements of Refs. 26 and 27 to thermal conductivity values. The same overall model should be assumed by the users of the present thermal conductivity equation to get prediction performances consistent with those of this study. The effects of using the Tillner-Roth EoS [1] over the whole P, T plane are discussed in Section 4.6.

Table III. Parameters of Eq. (12)

i	g_i	h_i	n_i	i	g_i	h_i	n_i
1	0.0	1.0	8.52652769	6	0.5	8.0	-1.61230375×10^7
2	0.0	2.0	1.67965784	7	1.0	8.0	1.52391557×10^7
3	1.5	9.0	0.00147845650	8	1.5	0.0	2.11072507
4	2.0	0.0	6.01649517	9	1.5	8.0	-4.79984974×10^6
5	0.0	8.0	5.68463574×10^6		n_c		0.195819321

4.2. Multiparameter Equation

The application of the optimization method to the final choice of primary datasets, see Section 3.3, led to the following equation:

$$\lambda_r(T_r, \rho_r) = \sum_{i=1}^{4} n_i T_r^{g_i} \rho_r^{h_i} + e^{-5\rho_r^2} \sum_{i=5}^{9} n_i T_r^{g_i} \rho_r^{h_i} + n_c \lambda_{r,ce}(T_r, \rho_r) \qquad (12)$$

with the coefficients and exponents reported in Table III; the analytical form of the term $\lambda_{r,ce}(T_r, \rho_r)$ is given by Eqs. (5) and (6) with the parameters from Table IV.

The proposed equation, Eq. (12), can be used inside the limits of validity given in Table V; the extrapolation of the equation far outside these limits, in particular, at low temperatures and at high pressures, should be avoided because it may result in unreliable calculated values. Even if the primary data do not cover the entire extension of the stated limits, see Fig. 1, a regular contour was assumed for the range of validity and this assumption will be discussed in Section 4.5.

Some thermal conductivity points generated from the new equation are given in Table VI as sample values for checking computer codes.

4.3. Validation of the New Thermal Conductivity Equation

The new thermal conductivity equation was validated in detail with respect to both primary and secondary data; the results are reported in the following. The same statistical indexes already defined in Eq. (8) are assumed also for the validation of the equation.

The deviations of Eq. (12) with respect to all the available experimental data within the limits of validity indicated in Table V are presented in Table I; the number of the considered points for each dataset is reported in the column 'NPT range'.

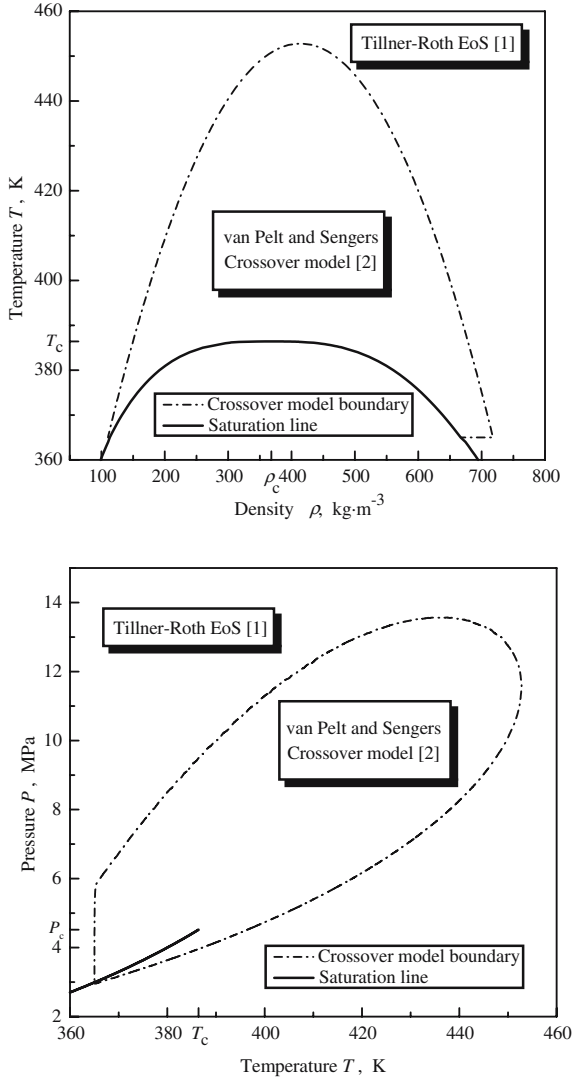

Fig. 2. Boundaries of the application region of the crossover model [2].

Figure 3 shows the deviations of the primary data from the thermal conductivity equation; the size of the symbols is related to the magnitude of the deviations. The deviations with respect to the primary data in the low-density region, here conventionally bounded by $P < 0.12$ MPa, are presented in Fig. 4. Furthermore, the distribution of the deviations of

Table IV. Parameters of the Critical Term, Eqs. (5) and (6)

i	a_i	i	a_i
1	1.0	7	0.30131
2	7.51327	8	0.92860
3	0.0	9	0.98794
4	0.30	10	0.085
5	0.30	11	0.15
6	0.46111	12	0.05

Table V. Validity Limits of Eq. (12)

T (K)	220–460
P (MPa)	$\leq$55

the experimental points of the primary datasets from Eq. (12) is shown in Fig. 5 as a function of pressure for several increments of temperature. The dashed-dotted lines represent the deviation of the conventional equation [17] with respect to Eq. (12), and for each figure, the temperature at which the two equations are compared is the mean value of the indicated range.

The good performance of the new thermal conductivity equation for R152a is evidenced by Table I and Figs. 3–5. The accuracy of the equation for the primary data, roughly indicated by the AAD values, approximately equals the level of the claimed experimental uncertainty in each of the three regions. The bias values differ slightly from zero in the vapor, liquid, and supercritical regions; this means that the equation is centered with respect to the data themselves in those regions. The low values of AAD and bias for the overall primary dataset is a further demonstration of the good behavior of the equation.

Table VI. Thermal Conductivity Values Generated from Eq. (12)

T (K)	P (MPa)	ρ (kg·m^{-3})	λ (mW·m^{-1}·K^{-1})	T (K)	P (MPa)	ρ (kg·m^{-3})	λ (mW·m^{-1}·K^{-1})
220	0.1	1069.307	137.102	386.8	4.55	319.853	107.366
298.15	0.1	2.72166	13.8391	387.5	4.6	306.6176	78.4462
330	0.1	2.44270	16.6631	300	15	938.613	111.573
460	0.1	1.73469	30.8300	400	25	764.052	88.8498
250	1.0	1010.73	123.916	250	40	1068.586	143.771
350	3	748.196	81.9418	460	55	779.677	97.5814

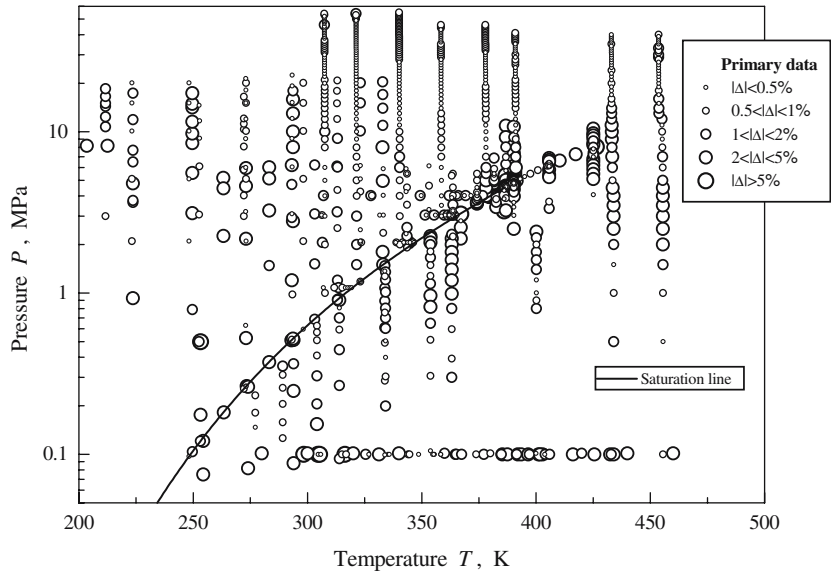

Fig. 3. Deviations between Eq. (12) and the experimental points in the primary datasets.

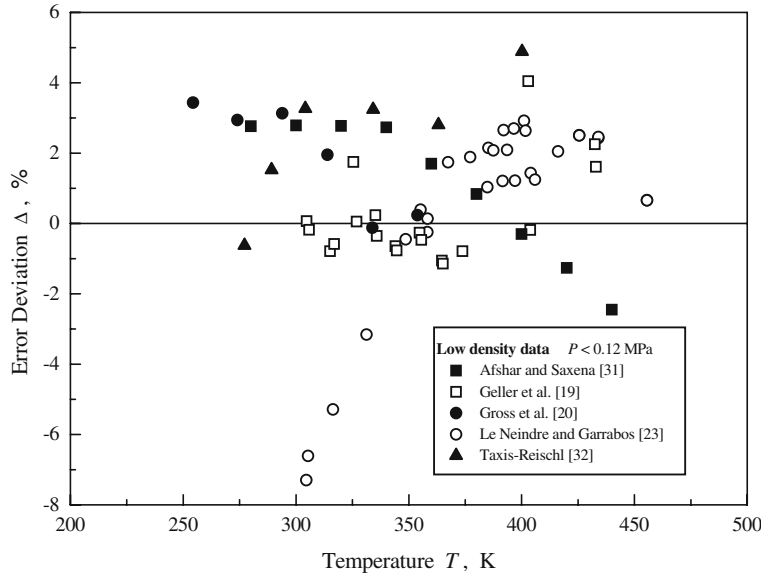

Fig. 4. Deviations between Eq. (12) and the primary experimental points in the low-density region.

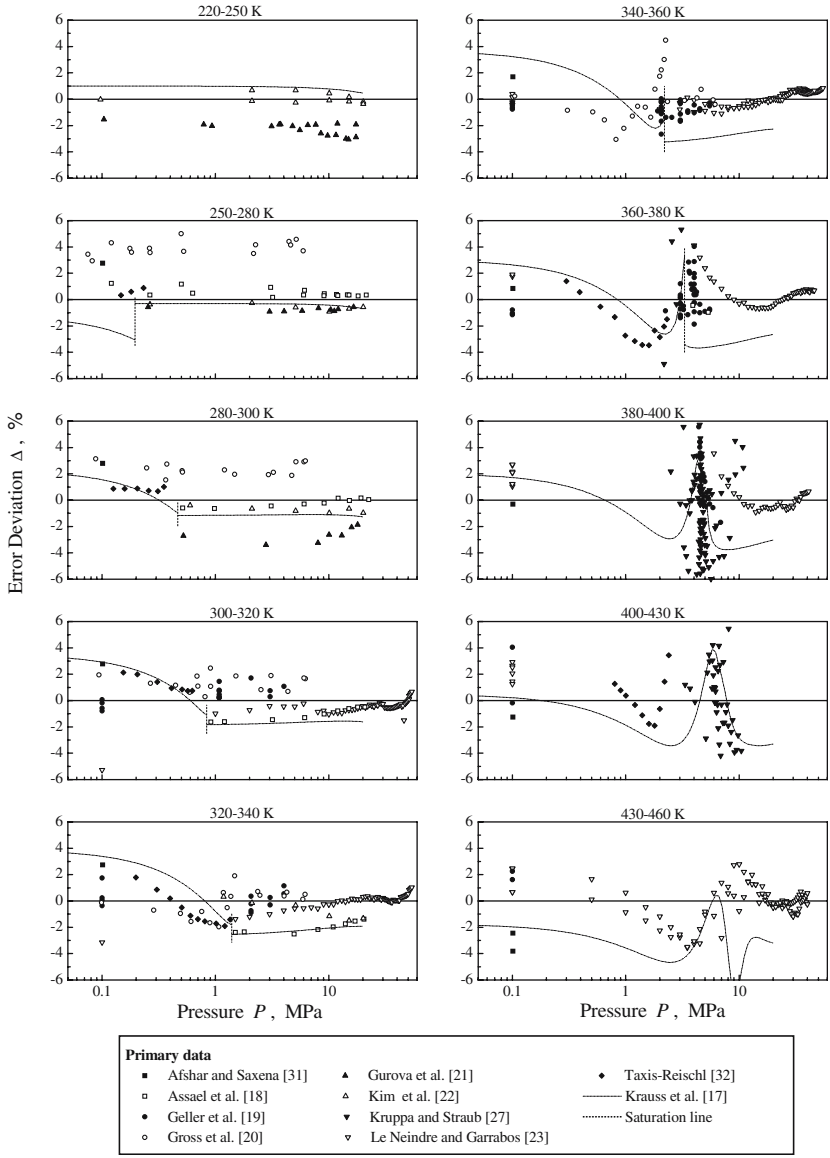

Fig. 5. Deviations of Eq. (12) with respect to all experimental points of the primary datasets and with respect to the conventional equation [17] as a function of pressure for several increments of temperature.

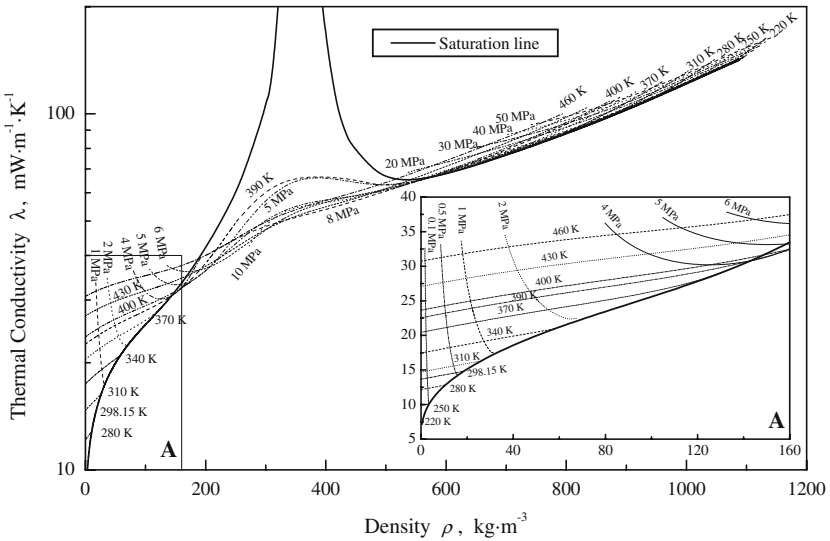

Fig. 6. Representation of Eq. (12) on a λ, ρ plane for several isotherms and isochors.

Table I shows that some experimental datasets are affected by high systematic errors, particularly the thermal diffusivity datasets at saturated conditions [26, 27]. Moreover, some inconsistencies among different sources are evidenced in Figs. 4 and 5, but the thermal conductivity equation seems to provide a reasonable balance among the data.

4.4. Behavior of the Thermal Conductivity Surface

Some isotherms and isobars calculated from the new thermal conductivity equation, Eq. (12), are plotted on a λ, ρ plane in Fig. 6. A magnification for the vapor region at pressures lower than 6 MPa is also shown. One can see that the surface is very regular, confirming once more the reliability of the equation. The steep trends of the vapor and liquid lines at saturated conditions are due to the infinity limit of the thermal conductivity at the critical point. The contribution of the critical term can be seen also in the plots of the isotherms and isobars at temperatures or pressures near the respective critical values.

For the near-critical region a more detailed representation is shown in Fig. 7, where some isotherms are plotted together with the experimental data from Kruppa and Straub [27] approximately at the same temperatures. The satisfactory representation of the experimental data confirms

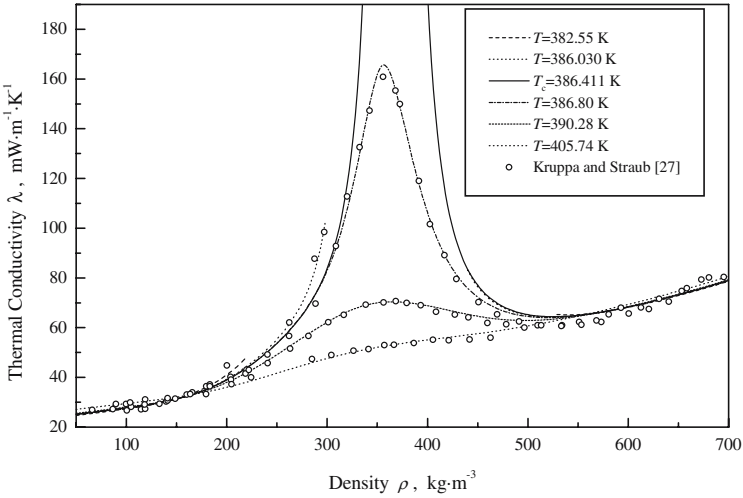

Fig. 7. Representation of Eq. (12) on a λ, ρ plane for the near-critical region.

that the critical term, Eqs. (5) and (6), is suitable to represent the critical enhancement of the thermal conductivity.

4.5. Discussion on the Limits of Validity and the Equation Accuracy

From Fig. 1, it is evident that the primary data do not uniformly fill a single regular range, both in temperature and in pressure, and then an irregular contour for the validity range should be selected for sake of precision. In fact, one can see, for instance, a total lack of data for the compressed liquid at $T < 300\,\mathrm{K}$ and $P > 25\,\mathrm{MPa}$, a scarcity of data for the liquid at $T < 250\,\mathrm{K}$ and $P < 1\,\mathrm{MPa}$, and no data for the vapor at $T < 250\,\mathrm{K}$.

In spite of these missing data, the plot reporting sections of the new equation, Fig. 6, shows that the trends of the equation in the regions where experimental data are not available are regular and they are consistent with the expected behavior. This indicates that the equation can be used in these areas as well, even if the equation accuracy cannot be verified in these regions for a lack of experimental data.

Some other considerations should also be noted. For the liquid, particularly at high pressures, a large pressure variation corresponds to a limited density variation, as can be seen from Fig. 6; therefore, since the equation variables are T and ρ, a strong extrapolation in pressure may correspond to a small extrapolation in density and then the accuracy level of the thermal conductivity equation is not significantly reduced. On the

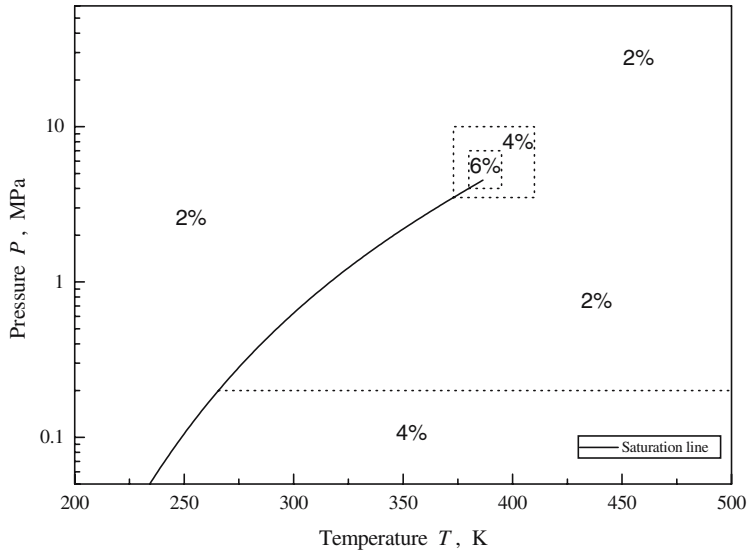

Fig. 8. Estimated accuracy of Eq. (12).

other hand, the dependence of the thermal conductivity on temperature for the vapor at low pressures is regular and smooth, and consequently in this region, where data are missing, the interpolation and the extrapolation are sufficiently reliable.

Considering all these reasons, the range of validity of the proposed thermal conductivity equation assumes a rectangular shape in the T, P plane; see Table V.

Figure 8 shows the estimated accuracy of the equation. In the vapor phase at pressures lower than 0.2 MPa, there are some inconsistencies among different datasets, as evidenced by Fig. 4, and the accuracy is consequently set at 4%. For the vapor phase at higher pressures, for the liquid phase, and for the supercritical region the data situation is better and the uncertainty is estimated to be 2%. In the region around the critical point, the precision of the equation is lower: for approximate ranges of temperature between 373 and 410 K and of pressure between 3.5 and 10 MPa the estimated uncertainty is 4%, while for temperatures between 380 and 395 K and for pressures between 4 and 7 MPa it is 6%.

4.6. Consequences of the Simplification of the Thermodynamic Model

In Section 4.1, it was stated that the density values required by Eq. (12) must be calculated with the van Pelt and Sengers model [2] inside

the critical region and with the Tillner-Roth EoS [1] outside such a region. The crossover model from Ref. 2 is necessary because the EoS from Ref. 1 is not suitable for a precise representation of the thermodynamic properties in the critical region. For instance, it locates the critical point of R152a at $T_c = 386.5315\,\mathrm{K}$, $P_c = 4.5269\,\mathrm{MPa}$, and $\rho_c = 359.355\,\mathrm{kg \cdot m^{-3}}$, which are different from the values reported in Table II.

A user not particularly experienced in numerical methods and in scaled fundamental equations of state can have difficult problems in understanding a crossover model and in implementing it into computer software. As a consequence, he may decide to use the Tillner-Roth equation [1] over the complete T, P plane, including also the critical region.

The effect of this simplification is shown in Fig. 9. At given temperature and pressure inside the validity range of the crossover model, the density is calculated with both the Tillner-Roth EoS [1] and the van Pelt and Sengers model [2]; the corresponding thermal conductivity values are obtained from Eq. (12), and the error introduced by the use of the Tillner-Roth EoS is calculated with

$$\Delta_{TR} = \frac{\lambda(T, \rho_{TR}) - \lambda(T, \rho_{vPS})}{\lambda(T, \rho_{vPS})} \tag{13}$$

where ρ_{TR} stands for the density calculated from the Tillner-Roth EoS and ρ_{vPS} for the density calculated from the van Pelt and Sengers model.

The contour lines at fixed values of Δ_{TR} are plotted for the P, T and T, ρ planes in Fig. 9: in the second case, the abscissa variable is the density from the Tillner-Roth EoS ρ_{TR}. From the diagrams, one can see that the error introduced by using the Tillner-Roth EoS instead of the crossover model exceeds 1% only in a very narrow region close to the critical point. The simplification of the thermodynamic model is therefore allowed when a decrease of accuracy, as shown in Fig. 9, can be accepted.

5. COMPARISON WITH THE CONVENTIONAL EQUATION

The thermal conductivity equation proposed by Krauss et al. [17] in a conventional format was used for comparison. The required thermodynamic properties were calculated with the same thermodynamic model used for the present equation, as done in the original publication [17]. The comparison with the new equation is made within the validity limits of this conventional equation, which are narrower. The results are reported in Table VII.

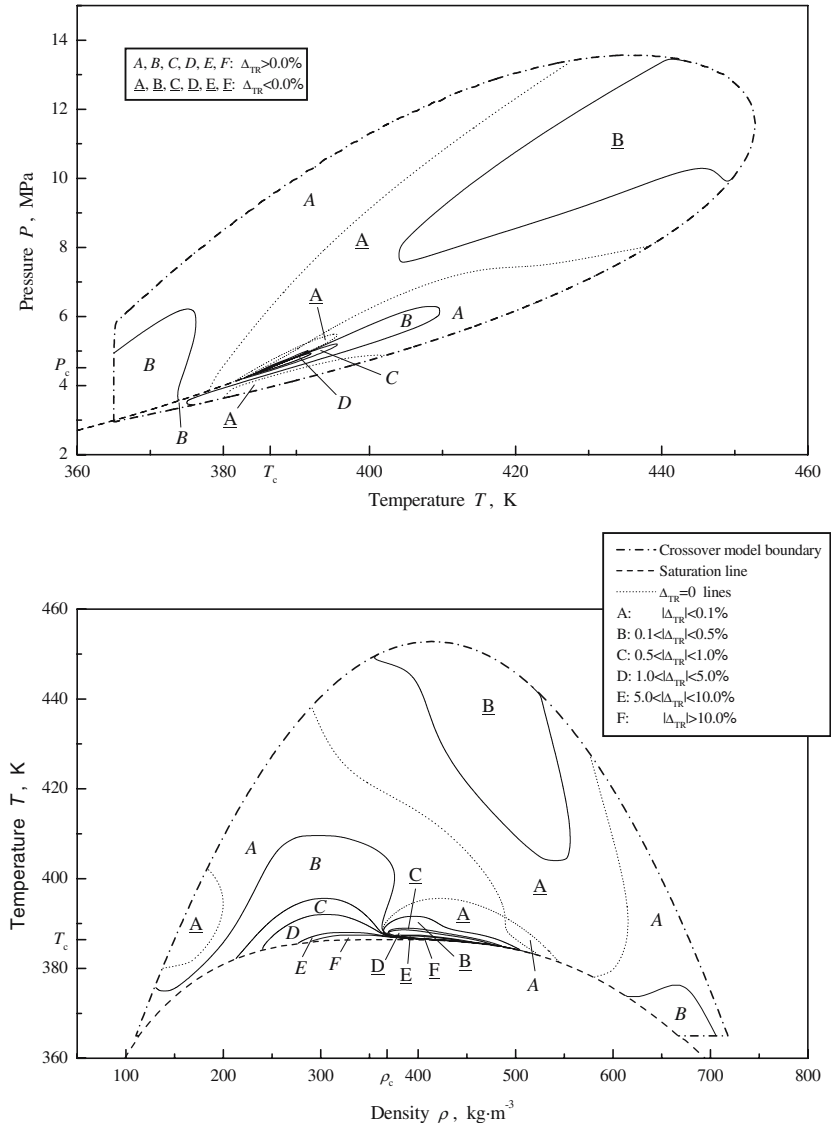

Fig. 9. Maps of the error introduced in Eq. (12) using the Tillner-Roth EoS [1] instead of the van Pelt and Sengers model [2] in the critical region.

Table VII. Comparison of the Performance of the New Thermal Conductivity Equation, Eq. (12), with Respect to the Krauss et al. [17] Conventional Equation. Data are within the Limits of Validity of the Conventional Equation

				Equation (12)			Krauss et al. [17]			
Ref.	First Author	Phase	NPT	AAD (%)	Bias (%)	MAD (%)	AAD (%)	Bias (%)	MAD (%)	Class Eq. (12)
Liquid phase										
18	Assael	l	35	0.85	−0.47	2.51	0.73	0.72	1.46	I
18	Assael	sl	5	1.24	−0.61	2.39	0.64	0.64	1.07	I
19	Geller	l	108	1.56	0.73	10.50	3.58	3.58	11.21	I
20	Gross	l	44	1.96	1.86	5.01	3.37	3.37	4.86	I
21	Gurova	l	23	1.98	−1.98	3.40	1.50	−1.48	3.05	I
21	Gurova	sl	3	1.60	−1.60	2.71	1.09	−1.09	1.84	I
22	Kim	l	20	0.63	−0.63	1.49	0.54	0.33	2.03	I
22	Kim	sl	4	0.28	−0.12	0.40	1.05	0.85	2.55	I
23	Le Neindre	l	101	0.58	−0.27	4.11	2.05	2.05	6.61	I
	Primary		343	1.20	0.15	–	2.41	2.17	–	
24	Grebenkov	l	72	5.44	−5.44	9.96	3.20	−3.20	6.90	II
25	Gross	sl	24	3.93	3.93	6.31	4.81	4.81	7.48	II
26	Kraft	sl	16	5.13	−0.52	25.44	3.03	0.04	20.76	II
27	Kruppa	l	27	6.80	−4.69	18.11	5.76	−1.87	13.80	II
27	Kruppa	sl	49	9.99	7.22	64.79	7.05	1.93	24.63	II
28	Tsvetkov	l	6	1.77	1.77	2.37	2.17	2.17	2.68	II
29	Vargaftik	l	33	0.96	0.24	5.91	2.62	2.62	6.84	II
30	Yata	l	15	3.87	−2.23	9.50	2.92	−0.71	6.41	II
	Total		585	3.00	−0.07	–	3.18	1.30	–	
Vapor phase										
31	Afshar	v	9	1.96	1.07	2.79	1.13	−0.50	2.39	I
19	Geller	v	19	0.91	0.15	4.05	3.30	−2.36	4.23	I
20	Gross	v	40	1.70	0.67	4.48	2.62	0.90	8.90	I

Table VII. Continued.

Ref.	First Author	Phase	NPT	Equation (12) AAD (%)	Equation (12) Bias (%)	Equation (12) MAD (%)	Krauss et al. [17] AAD (%)	Krauss et al. [17] Bias (%)	Krauss et al. [17] MAD (%)	Class Eq. (12)
27	Kruppa	v	46	2.99	0.27	8.23	3.66	0.18	11.83	I
23	Le Neindre	v	37	2.44	−0.19	9.12	2.80	−0.71	11.64	I
32	Taxis-Reischl	v	54	1.53	0.08	4.89	1.26	0.11	6.34	I
	Primary		205	2.02	0.24	–	2.53	−0.13	–	
33	Hammerschmidt	v	4	4.55	3.64	8.24	2.54	1.80	5.07	II
26	Kraft	sv	6	7.39	7.39	27.32	5.89	4.75	24.76	II
27	Kruppa	sv	30	17.51	−16.11	90.52	14.44	−13.90	51.78	II
29	Vargaftik	v	9	2.37	−2.37	5.37	3.53	−3.53	4.95	II
34	Yin	v	14	7.16	−7.16	8.67	9.86	−9.86	12.32	II
	Total		268	4.19	−1.85	–	4.35	−2.15	–	
Supercritical region										
27	Kruppa	sc	103	2.31	−0.64	6.28	2.89	−0.65	8.71	I
23	Le Neindre	sc	33	1.03	0.28	3.54	3.42	3.08	6.47	I
	Primary		136	2.00	−0.42	–	3.02	0.26	–	
24	Grebenkov	sc	6	8.82	−8.82	9.51	5.22	−5.22	5.89	II
	Total		142	2.29	−0.77	–	3.11	0.03	–	
Overall										
	Primary		684	1.60	0.06	–	2.57	1.10	–	
	Total		995	3.22	−0.65	–	3.49	0.19	–	

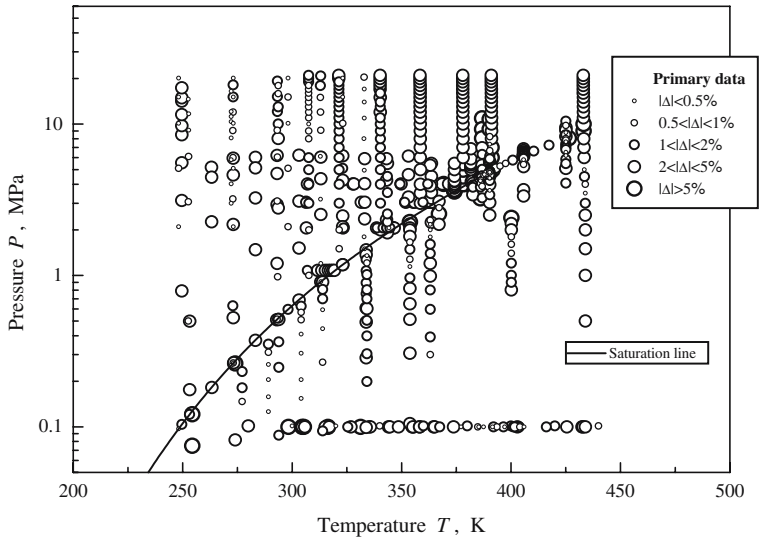

Fig. 10. Deviations between the conventional equation [17] and the experimental points in the primary datasets.

The AAD and bias values for the primary data show that the new equation, Eq. (12), is superior to the conventional one [17] for the single-phase regions and for the whole surface. In particular, a larger difference is verified for the liquid primary data, for which the present equation shows good behavior and the conventional one has a double AAD value. Moreover, the conventional equation is shifted with respect to the data, as evidenced by the high bias value. Also in the supercritical region the new equation performs better than the conventional one. Globally, the conventional equation has a lower accuracy and it seems to be not well centered with respect to the experimental data.

A graphic comparison between the two equations and with respect to experimental data is reported in Fig. 5. The deviations of the conventional equation from the present primary data are shown in Fig. 10, which corresponds to Fig. 3 for the new equation. In Fig. 10, only the experimental points inside the range of validity of the conventional equation were reported, even if the scales of the axes are the same as Fig. 3 to facilitate the comparison.

A 'practical' element of comparison has to be stressed: from the user's point of view, the implementation of the conventional equation into computer software is quite difficult, due to the complexity of the critical enhancement model. In fact, the calculation of the critical enhance-

ment term in the conventional format requires also the viscosity value, the solution of cubic and quartic equations in complex variables, the solution of linear systems with complex coefficients and variables, the handling of equations with complex parameters, and values of different thermodynamic properties such as density, isobaric and isochoric heat capacities, and isothermal compressibility.

A user not particularly familiar with these subjects could choose either to take some simplified equation for the critical enhancement or not to calculate it at all. The effect of these simplifications on the accuracy of the model could be quite pronounced.

Moreover, the crossover EoS [2] is very difficult to handle, because it implies the solution of some implicit equations. On the other hand, the alternative use of the Tillner-Roth EoS [1] also in the critical region would probably result in an inaccurate description of the critical enhancement in the conventional format, because the calculation of this term requires properties like c_p and c_v whose trends in the critical region are not followed by the Tillner-Roth EoS.

On the contrary, the implementation of the thermal conductivity model proposed in the present paper is quite simple, since it is composed of just a few explicit equations involving only basic mathematics. In the critical region the crossover model is needed for the calculation of the density, which is the only required thermodynamic quantity, but if the Tillner-Roth EoS is used in this region the introduced error is quite small, apart from a narrow region around the critical point, see Fig. 9.

6. CONCLUSIONS

A heuristic modeling technique, directly based on the available thermal conductivity experimental data, was applied to develop a new thermal conductivity equation for R152a. The technique is composed of an optimization method for the functional form of multiparameter equations of state, developed by Setzmann and Wagner [16], and by a nonlinear regression method. An analytical expression to represent the thermal conductivity critical enhancement was set up and included in the equation.

The new multiparameter thermal conductivity equation shows an AAD value of 1.32% with respect to the selected 939 primary data, which represents a significant improvement in performance compared to the existing equation in a conventional format [17]. In fact, considering only 684 primary data inside the range of validity of the conventional equation, the new equation reaches an AAD of 1.60% and the conventional one gives an AAD of 2.57%. Also the bias values of the new equation are close to zero assuring the absence of systematic shifts.

Due to its heuristic and non-theoretical nature, the proposed modeling method can be also used for experimental data screening, and it can be adopted to effectively represent the whole thermal conductivity surface of a fluid within the uncertainty of the experimental data.

REFERENCES

1. R. Tillner-Roth, *Int. J. Thermophys.* **16**:91 (1995).
2. A. van Pelt and J. V. Sengers, *J. Supercrit. Fluids* **8**:81 (1995).
3. P. Marchi, G. Scalabrin, and M. Grigiante, *Int. J. Thermophys.* (in press).
4. G. Scalabrin, P. Marchi, and R. Span, *J. Phys. Chem. Ref. Data* **35**:839 (2006).
5. G. Scalabrin, P. Marchi, and F. Finezzo, *Fluid Phase Equilib.* **245**:37 (2006).
6. J. Millat, J. H. Dymond, and C. A. Nieto de Castro, eds., *Transport Properties of Fluids. Their Correlation, Prediction and Estimation* (Cambridge University Press, Cambridge, 1996).
7. A. Laesecke, R. Krauss, K. Stephan, and W. Wagner, *J. Phys. Chem. Ref. Data* **19**:1089 (1990).
8. G. Cristofoli, L. Piazza, and G. Scalabrin, *Fluid Phase Equilib.* **199**:223 (2002).
9. G. Scalabrin, L. Piazza, and V. Vesovic, *High Temp.-High Press.* **34**:457 (2002).
10. G. Scalabrin and G. Cristofoli, *Int. J. Refrig*. **26**:302 (2003).
11. G. Scalabrin and G. Cristofoli, *Int. J. Thermophys*. **24**:1241 (2003).
12. G. Scalabrin, G. Cristofoli, and D. Richon, *Fluid Phase Equilib.* **199**:265 (2002).
13. G. Scalabrin, G. Cristofoli, and D. Richon, *Fluid Phase Equilib.* **199**:281 (2002).
14. G. Scalabrin, P. Marchi, and R. Span, *J. Phys. Chem. Ref. Data* (in press).
15. G. Scalabrin, P. Marchi, F. Finezzo, and R. Span, *J. Phys. Chem. Ref. Data* (in press).
16. U. Setzmann and W. Wagner, *Int. J. Thermophys*. **10**:1103 (1989).
17. R. Krauss, V. C. Weiss, T. A. Edison, J. V. Sengers, and K. Stephan, *Int. J. Thermophys.* **17**:731 (1996).
18. M. J. Assael, L. Karagiannidis, and W. A. Wakeham, *Proc. ASME Winter Ann. Meet.* (New Orleans, 1993), p. 1.
19. V. Z. Geller, G. V. Zaporozhan, and S. V. Ilyushenko, *Prom. Teplotekh*. **4**:77 (1992).
20. U. Gross, Y. W. Song, and E. Hahne, *Int. J. Thermophys*. **13**:957 (1992).
21. A. N. Gurova, C. A. Mardolcar, and C. A. Nieto de Castro, *Int. J. Thermophys*. **20**:63 (1999).
22. S. H. Kim, D. S. Kim, M. S. Kim, and S. T. Ro, *Int. J. Thermophys*. **14**:937 (1993).
23. B. Le Neindre and Y. Garrabos, *High Temp.-High Press.* **34:**307 (2002).
24. A. J. Grebenkov, Yu. G. Kotelevsky, V. V. Saplitza, O. V. Beljaeva, T. A. Zajatz, and B. D. Timofeev, *Proc. Joint Meet. IIR Commun. B1, B2, E1, E2* (Padova, Italy, 1994), p. 419.
25. U. Gross, Y. W. Song, and E. Hahne, *Fluid Phase Equilib.* **76**:273 (1992).
26. K. Kraft and A. Leipertz, *Int. J. Thermophys*. **15**:791 (1994).
27. B. Kruppa and J. Straub, *Int. J. Thermophys*. **18**:807 (1997).
28. O. B. Tsvetkov, Yu. A. Laptev, and A. G. Asambaev, *Int. J. Thermophys*. **17**:597 (1996).
29. N. B. Vargaftik, L. P. Filippov, A. A. Tarzimanov, and E. E. Totskii, *Handbook of Thermal Conductivity of Liquids and Gases* (CRC Press, Boca Raton, Florida, 1994).
30. J. Yata, M. Hori, T. Kurahashi, and T. Minamiyama, *Fluid Phase Equilib.* **80**:287 (1992).
31. R. Afshar and S. C. Saxena, *Int. J. Thermophys*. **1**:51 (1980).
32. B. Taxis-Reischl, *Thesis* (University of Stuttgart, Stuttgart, 1994).
33. U. Hammerschmidt, *Int. J. Thermophys*. **16**:1203 (1995).

34. J. M. Yin, J. X. Guo, Z. Y. Zhao, L. C. Tan, and M. Zhao, *Fluid Phase Equilib.* **80**:297 (1992).
35. H. Preston-Thomas, *Metrologia* **27**:3 (1990).
36. J. V. Sengers, *Int. J. Thermophys*. **6**:203 (1985).
37. P. J. Mohr and B. N. Taylor, *Rev. Mod. Phys*. **72**:351 (2000).
38. P. Becker, H. Bettin, H.-U. Danzebrink, M. Glaser, U. Kuetgens, A. Nicolaus, D. Schiel, P. De Bievre, S. Valkiers, and P. Taylor, *Metrologia* **40**:271 (2003).
39. R. Schmidt and W. Wagner, *Fluid Phase Equilib.* **19**:175 (1985).
40. R. Span, *Multiparameter Equations of State* (Springer, Berlin, 2000).
41. E. W. Lemmon and R T. Jacobsen, *Int. J. Thermophys*. **25**:21 (2004).